CONF-790518--3

NOVEL MEASUREMENT OF PROTON DISTRIBUTION AND SITE ENERGIES IN METAL HYDRIDES

E. L. Venturini and P. M. Richards

Sandia Laboratories, Albuquerque, New Mexico 87185

Abstract

The low temperature electron spin resonance (ESR) spectrum of dilute Er in ScH_x and YH_x powders contains distinct signals which are due to the presence of octahedral as well as tetrahedral protons in the vicinity of the Er ions. The occupation probability for the octahedral protons is determined from the ESR signal intensities, and its variation with hydrogen-to-metal ratio x is explained by a lattice-gas calculation, yielding information about bulk proton distribution and relative site energies in these materials.

Introduction

In this paper we show that the low temperature electron spin resonance (ESR) spectrum of dilute Er in ScH_x and YH_x powders provides microscopic information concerning lattice location, net charge, site energy and associated occupation probability for bulk protons which are of fundamental importance in understanding these materials and improving their characteristics for specific applications. Each ESR spectrum contains three distinct signals associated with the Er ion (substituting on a host metal atom site) having zero, one or two protons on next-nearest neighbor octahedral (O) sites (see Figure 1). The occupation probability for O-sites adjacent to an Er ion versus the bulk hydrogen-to-metal ratio x is determined from integrated intensities of these signals and can be explained by a lattice-gas model.

The inset in Figure 1 shows an Er ion residing on a metal atom site in the face-centered-cubic dihydride lattice.[1] The eight nearest-neighbor protons shown as solid circles occupy tetrahedral (T) sites and form a simple cube around the Er, while

the six next-nearest-neighbor positions are O-sites shown as open circles forming an octahedron. The bulk O-sites are primarily vacant in bulk ScH_x and YH_x when $x < 2$. The ESR data shows that as x approaches 2, however, an appreciable number of Er impurity ions have a proton on O-site 1 (or one of the five equivalent locations), other Er ions have protons on both O-sites 1 and 2, while the remainder have no neighboring octahedral protons. The lattice-gas model which explains the occupation of these sites next to an Er ion yields additional information about proton distribution in the host hydride.

A particularly useful result obtained by fitting the lattice-gas model to the ESR data is the fraction of bulk O-sites filled by protons at a given value of x. In the case of ScH_x this fraction is less than 0.5% at $x = 2$ in agreement with the fact that Sc does not form a trihydride at ordinary pressures.[1] This result differs strongly from recent nuclear magnetic resonance (NMR) second moment measurements [2] on protons in ScH_x indicating that up to 30% of the bulk O-sites are filled at $x = 1.9$. The ESR results reported here should be more reliable since, in contrast to proton NMR, we observe separate resonances associated with O-site occupation next to an Er. The ESR data for Er in YH_x show that approximately 8% of the bulk O-sites are filled when $x = 2$. The ESR technique can thus be a powerful means of determining microscopic properties and phase boundaries of hydrides.

ESR Spectrum and Analysis

The derivative absorption ESR powder spectrum for 0.1% Er in $ScH_{1.993}$ taken at 2 K and 9.8 GHz is shown in Figure 1. Samples for this study were prepared by arc-melting the Er into specially purified Sc, then loading with hydrogen in a modified Sieverts' apparatus, and finally grinding the metal into a fine powder for the ESR measurements. The hydrogen-to-metal ratio x was determined volumetrically, and confirmed gravimetrically to better than 1%. The solid line in Figure 1 is the experimental curve, and the dashed line is the calculated ESR powder pattern for three distinct Er ion sites, one with cubic symmetry and two with axial symmetry. We have included the known

hyperfine lines for Er ions in a cubic site.[3] The main signal at 1035 Oe has a g-factor of 6.744±0.01, consistent with a Γ_7^1 ground state for trivalent Er in a cubic crystal field. If this field is produced by the cube of T-site protons, we can conclude that they are negatively charged.[4]

In addition to the main isotropic resonance and its eight hyperfine lines there are two resonances in Figure 1 associated with Er ions in distinct axial sites. Axial resonances in a powder sample are characterized by a positive peak and a "normal" derivative signal corresponding to $g_{\parallel}$ and $g_{\perp}$ for applied magnetic fields along and normal to the axial symmetry direction, respectively. In Figure 1 the two axial signals are identified by *superscripts 1 and 2*. The excellent fit has been obtained with the following adjustable parameters: a common lineshape asymmetry [5] for all signals, five g-factors, three isotropic linewidths and three intensities for the isotropic and two axial lines, respectively.

Referring to the inset in Figure 1, there are two simple ways to change the site symmetry of the Er ion from cubic to axial: a) remove a T-site proton from the nearest-neighbor cube or b) add a proton to one of the next-nearest-neighbor O-sites. Since the axial signals increase strongly with x (see Figure 2), we choose the latter, and conclude that the Er ions in ScH_x and YH_x are surrounded by eight T-site protons for all x in the dihydride single phase region (in agreement with recent Mossbauer measurements [6] on Er in ZrH_x). To strengthen this choice we have calculated the axial crystal field values needed to split the cubic g-factor into the values for the axial resonance with superscript 1. The value of axial field strength determined in this calculation was then doubled, and the g-factors predicted for twice the axial perturbation agreed with those measured for the axial resonance with superscript 2 within experimental error. This calculation plus the axial symmetry of resonance 2 requires that the two adjacent O-site protons reside on opposite sides of the Er (sites 1 and 2 in Figure 1). Orthorhombic or lower site symmetry for the Er has a totally different ESR

powder pattern which we have measured for Er in YH_x with $x > 2.2$. The above interpretation of the ESR spectrum in Figure 1 implies that it is energetically favorable for the second octahedral proton next to an Er ion to reside on O-site 2 rather than one of the four O-sites in the plane immediately below site 1. For Er in YH_x the ESR spectrum is similar to that in Figure 1 with somewhat larger splittings in the axial g-factors.

By comparing the integrated intensities of each axial signal with that of the isotropic line, we can determine the relative probability of one or two adjacent O-site protons compared to zero octahedral protons. In Figure 2 we compare the fraction of Er ions with one neighboring O-site proton for YH_x (open circles) and ScH_x (solid circles) versus the hydrogen-to-metal ratio x. The samples were prepared to span the single phase region for both hosts. The most striking feature of these data is the rapid increase in Er ions with adjacent O-site protons near $x = 2$ for ScH_x in contrast to the gradual increase across the single phase region for YH_x. The lattice-gas calculation described below shows that this is a natural consequence of bulk O-site proton occupation which occurs in YH_x but not ScH_x.

Lattice-Gas Model

The observed dependence on x may be understood in terms of a lattice-gas model [7] which is equivalent to an Ising model in an applied field. The probability of an impurity ion having an adjacent O-site occupied normalized to the probability of having all O-sites vacant is given by

$$p_1 = 6\exp[-\beta^*(V_0'-\mu)] \qquad (1)$$

where $\beta^* = 1/k_B T^*$ and T^* is an effective "freeze out" temperature to be discussed below, V_0' is the energy of an O-site neighboring an impurity, μ is the chemical potential and there are 6 available sites. For impurity concentration $c \ll 1$ it is sufficient to determine μ by considering bulk proton site occupation, the equations for which are

$$c_T = \{\exp[\beta^*(U_T-\mu)] + 1\}^{-1}, \qquad c_O = \{\exp[\beta^*(U_O-\mu)] + 1\}^{-1} \tag{2}$$

$$c_O + 2c_T = x \tag{3}$$

where U_T and U_O are bulk T- and O-site energies, respectively, and interactions have been neglected. Here c_T and c_O, the fraction of each site occupied by protons, are functions of x because of Equation 3. In the absence of bulk O-site occupation we have

$$P_1 = \frac{Ax}{2-x} \tag{4}$$

where $A = 6\exp[\beta^*(U_T-V_O')]$.

The solid curve in Figure 2 gives a good fit to the ScH_x data (solid circles) with A = 0.0035. The fact that A/6 << 1 indicates that $V_O' > U_T$, i.e., it is still <u>energetically</u> favorable for a proton to occupy a bulk T-site as opposed to an O-site adjacent to an Er impurity, but there is a big gain in <u>free energy</u> with O-site occupation. This is because at x = 2 and low impurity concentration, one can increase entropy by the order of N by allowing a proton to move from one of the N bulk T-sites to an O-site near an Er.

The rapid increase in impurity O-site occupation near x = 2 for Er in ScH_x is a direct reflection of the lack of bulk O-site occupation. If bulk O-site occupation is included, Equation 4 becomes

$$P_1 = \frac{A[x-c_O(x)]}{2-x+c_O(x)} \tag{5}$$

where the solutions to Equations 2 and 3 give

$$c_O(x) = x - \frac{4x}{2+x+B(1-x)+\sqrt{\{[2-x+B(1-x)]^2+4Bx(3-x)\}}} \tag{6}$$

with $B = \exp[\beta^*(U_T-U_O)]$. The error bars on the ScH_x data in Figure 2 place an upper limit on c_O of 0.5% at x = 2 which implies $B < 10^{-5}$.

In contrast to ScH_x the YH_x data obviously cannot be explained by the one-parameter model in Equation 4 which neglects bulk O-site occupation. The dashed line in Figure 2 is a least-squares fit of Equation 5 with A = 0.0061 and B = 0.0040. This value of B allows substantial bulk O-site occupation below x = 2, and c_O is 8.4% at x = 2. This prevents a rapid rise in impurity O-site occupation in YH_x near x = 2, resulting in the gradual increase with x across the single phase region as shown.

Thermal equilibrium is established at the freeze out temperature $T^* = 1/k_B\beta^*$ rather than the low experimental temperature of 2 K. If we take T^* = 200 K [8] the values for A in both ScH_x and YH_x correspond to a difference of about 0.1 eV between Er O-site and bulk T-site energies, which may include mean field T-T and O-T interactions. In the case of YH_x the energy difference between bulk O-site and T-site protons is also about 0.1 eV, since A and B are comparable, which means that O-site energies in the bulk and next to an Er impurity are about the same. However, the upper limit of c_O = 0.5% at x = 2 in ScH_x implies a difference between bulk O-site and T-site proton energies of greater than 0.2 eV, so O-site occupation next to an Er ion is at least a factor of 2 less unfavourable energywise compared with the bulk hydride. This agrees with the observation that while the Er atom is too large for the ScH_x lattice and makes a substantial perturbation to neighboring site energies, it should be closely matched to the Y size in YH_x and thus create little disruption.

In conclusion, we have shown that dilute impurity ESR in metal hydrides is a sensitive probe of the proton behavior both adjacent to the impurity and in the bulk lattice. A simple lattice-gas model gives a very good explanation for the dependence of O-site proton occupation next to the impurity upon hydrogen-to-metal ratio x. This model can thereby be used to establish O-site occupation in the bulk hydride in a direct manner, providing a considerably more accurate determination than the more conventional NMR second-moment measurement, despite the perturbation introduced by the ESR impurity ion. By assuming a particular freeze out temperature for bulk proton diffusion, site

energies can be calculated. This method should be useful in a variety of problems relating to phases of hydrides and hydrogen in metals. It also may be applicable to the study of helium birth and subsequent release from tritides. The ESR signal versus time should provide a monitor of strain build-up in the lattice and possibly information about the location of He atoms.

References

1. Metal Hydrides, W. M. Mueller, J. P. Blackledge and G. G. Libowitz, eds. (Academic Press, New York, 1968), ch. 8 and 9.
2. H. T. Weaver, Phys. Rev. B5, 1663 (1972).
3. R. Chui, R. Orbach and B. L. Gehman, Phys. Rev. B2, 2298 (1970).
4. K. R. Lea, M. J. M. Leask and W. P. Wolf, J. Phys. Chem. Solids 23, 1381 (1962).
5. G. Feher and A. F. Kip, Phys. Rev. 98, 337 (1955).
6. G. K. Shenoy, B. D. Dunlap, D. G. Westlake and A. Dwight, J. de Physique 37 C6-129 (1976).
7. C. N. Yang and T. D. Lee, Phys. Rev. 87, 404 (1952).
8. The diffusion coefficient in Reference 2 suggests that at 20C K it takes on the order of 1 minute for a proton to diffuse the distance between impurity sites.

Figure Captions

Figure 1. Experimental (solid) and fitting (dashed) curves of ESR absorption derivative. Positions of the hyperfine lines from the main resonance as well as the axial lines $g_{\parallel,\perp}^{(1,2)}$ are shown. Inset shows tetrahedral (solid circles) and octahedral (open circles) proton sites surrounding Er in the host fcc lattice.

Figure 2. Relative number of Er ions with one octahedral proton normalized to number with no octahedral protons (cubic symmetry) versus x over the single phase region for ScH_x (solid circles) and YH_x (open circles). Curves are theoretical as explained in the text.

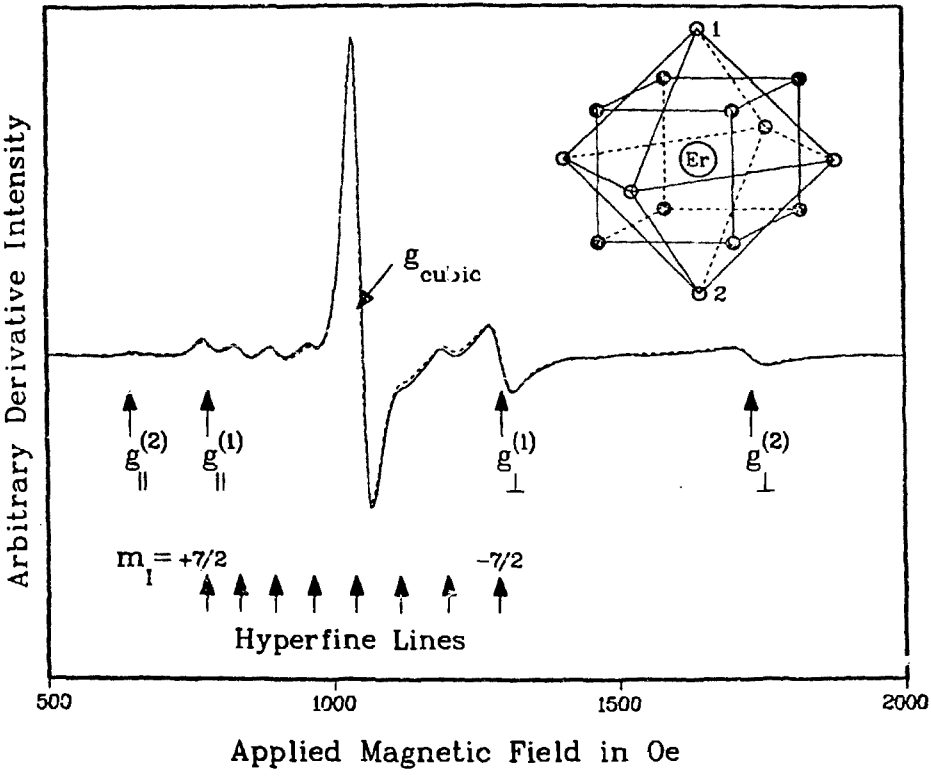

Venturini/Richards Figure 1

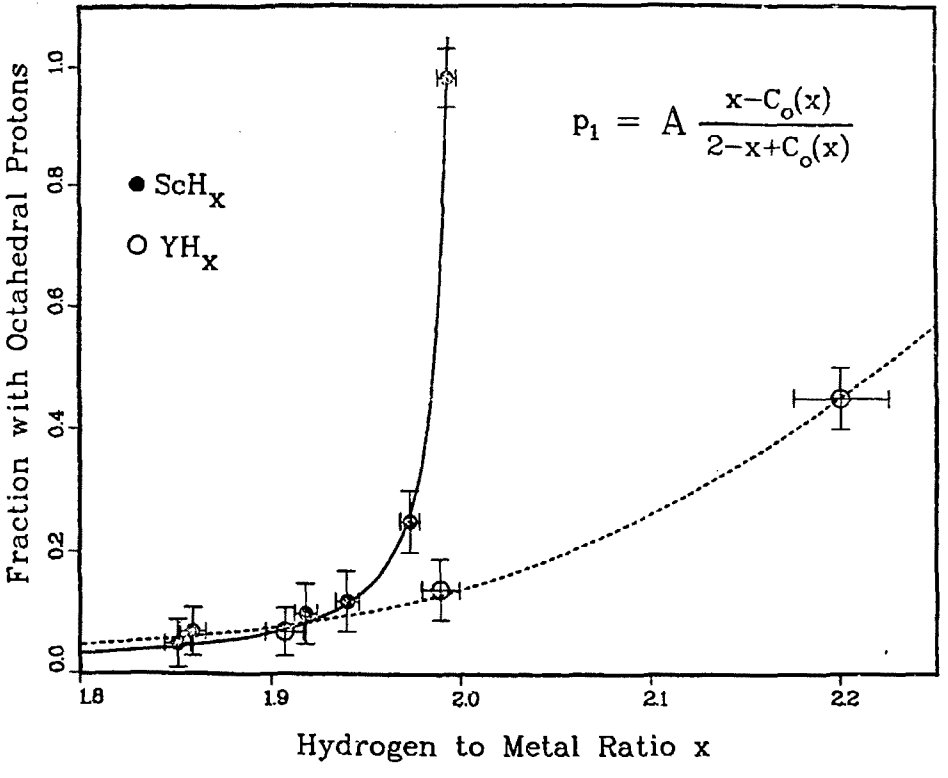

Venturini/Richards Figure 2